Spatially Localized Enhancement of Evanescent Coupling to Whispering-Gallery Modes at 1550 nm Due to Surface Plasmon Resonances of Au Nanowires

Elijah B. Dale, Deepak Ganta, Deok-Jin Yu, Bret N. Flanders, James P. Wicksted, and Albert T. Rosenberger, *Member, IEEE*

***Abstract*—We demonstrate a highly localized enhancement of evanescent coupling between a tapered optical fiber and a high-Q dielectric microresonator owing to the resonant evanescent excitation of localized surface plasmons of a gold nanowire placed on the microresonator's surface. This localized enhancement, at 1550 nm, is due to nanowire fragments that are confined to specific regions of the surface. The enhancement (of photon-tunneling probability) is measured by comparing properties of the whispering-gallery modes' throughput dips before and after deposition of the nanowire. The experimental results presented here show coupling enhancement by a factor of 10–700, depending on the position of fiber–microresonator contact in relation to the nanowire. These Au-nanowire-coated microresonators could provide enhanced sensitivity in various types of surface-plasmon-based gas, chemical, and biological-sensing applications within the telecommunication frequency bands.**

***Index Terms*—Electromagnetic coupling, microresonators, nanotechnology, plasmons.**

I. Introduction

LOCALIZED surface plasmon resonances (LSPRs) are collective coherent oscillations of electrons in metallic nanostructures. These resonances are known for their large near-field enhancement of the optical field. Cylindrical nanostructures (rods and wires) are of primary interest owing to the tunability of their longitudinal LSPRs, which redshift with increasing aspect ratio (length/diameter). In combination, these characteristics enable enhanced wavelength-tunable surface-plasmon-based resonant-sensing applications [1], [2]. LSPRs can be readily excited in nanostructure-coated dielectric waveguides, where confinement is due to total internal reflection, by the evanescent field of the guide at the dielectric interface. This in turn leads to strengthened field overlap with adjacent optical structures [3], and increased sensitivity to local environmental changes [4]. In this configuration, tapered-fiber waveguides have been previously used as probes for the analysis of vapor and liquid phases [4].

High-quality factor ($Q > 10^7$) whispering-gallery-mode (WGM) resonances in dielectric microresonators have been studied in many applications, ranging from optical add-drop filters to gas and chemical sensors [5]–[8]. Fused-silica microspheres may be fabricated by melting the end of an optical fiber in a hydrogen flame; low absorption and scattering losses are responsible for the high Q values. Light is efficiently coupled into WGMs by photon tunneling from an adjacent fiber that has been tapered by heating and stretching. The (typical) diameters of the tapered fiber and microsphere used here at a wavelength of 1550 nm are 3.5 and 620 μm, respectively. When the incident light is provided by a frequency-scanned laser, a WGM will be represented by a dip in the fiber throughput.

In the experiment reported here, LSPRs of fragments of a gold nanowire placed on the microsphere's surface are excited by the WGM's evanescent field. Resonant excitation of these LSPRs leads to localized evanescent-field enhancement, and thus, enhancement of the optical coupling between the microsphere and the tapered fiber. By monitoring the effect of the Au nanowire on the resonance dips in the fiber throughput, we can estimate the induced changes both in coupling and in intrinsic scattering and absorption losses. Previously, it has been shown that low-aspect-ratio ($\sim$4) Au nanorods homogeneously distributed over a microsphere's surface can lead to spatially uniform enhanced coupling [9] at a wavelength of 800 nm. In this paper, we now show that a nanowire can produce significant coupling enhancement localized in the vicinity of the nanowire at longer wavelengths, within the telecommunications window, due to the greater aspect ratio of the nanowire fragments. Our measurements show coupling enhancement (increase in photon-tunneling probability) by a factor of 10–700, depending on the location of the coupling point, accompanied by some increase in intrinsic loss due to the presence of scattering centers on the

Manuscript received June 30, 2010; revised September 7, 2010; accepted September 9, 2010. Date of publication October 28, 2010; date of current version August 5, 2011. This work was supported in part by the National Science Foundation (NSF) under Grant ECCS-0601362 and Grant EPS-0814361, and in part by the Oklahoma Center for the Advancement of Science and Technology under Grant AR072–066. The scanning electron microscope housed in the Oklahoma State University Microscopy Laboratory was supported by the NSF Major Research Instrumentation under Grant 0722410.

E. B. Dale, D. Ganta, D.-J. Yu, J. P. Wicksted, and A. T. Rosenberger are with the Department of Physics, Oklahoma State University, Stillwater, OK 74078–3072 USA (e-mail: ride70mustang@suddenlink.net; gantadeepak@gmail.com; deokjin.yu@okstate.edu; james.wicksted@okstate.edu; atr@okstate.edu).

B. N. Flanders is with the Department of Physics, Kansas State University, Manhattan, KS 66506–2601 USA (email: bret.flanders@phys.ksu.edu).

Color versions of one or more of the figures in this paper are available online at http://ieeexplore.ieee.org.

Digital Object Identifier 10.1109/JSTQE.2010.2078491

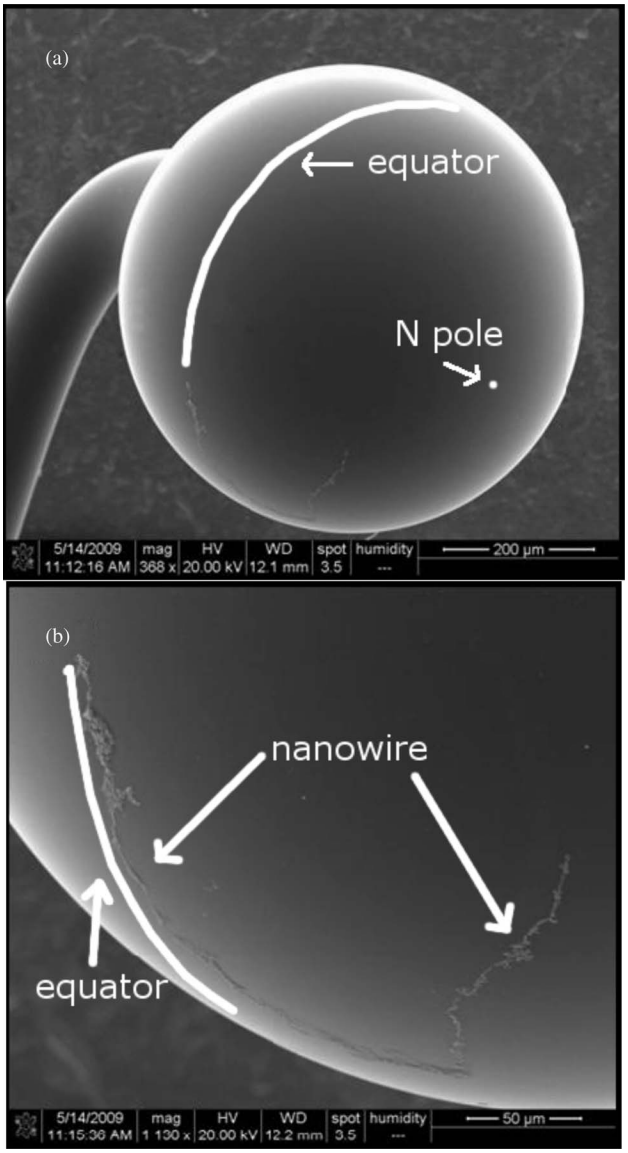

Fig. 1. SEM images of a microsphere on which a nanowire has been deposited. (a) Entire microsphere; scale bar is 200 μm. Approximate positions of the equator and the north (upper) pole are indicated. (b) Magnified image of the nanowire region seen in (a); scale bar is 50 μm. The equator and the two parts of the nanowire are denoted.

coated microsphere. These new results provide further confirmation of the interpretation of the enhancement observed [9] as being due to LSPR excitation. These Au-nanowire-coated microresonators could have potential applications in various types of gas, chemical, and biosensing.

II. Au Nanowire Growth, Placement, and Characterization

A gold nanowire is grown from Au nanorods, in a dielectrophoretic approach, between copper electrodes, as in [10]. This process has been slightly modified, by placing the electrodes on opposed linear stages, to allow for larger electrode gap distances to accommodate the microsphere's diameter. Also, both the magnitude and frequency of the ac potential between the

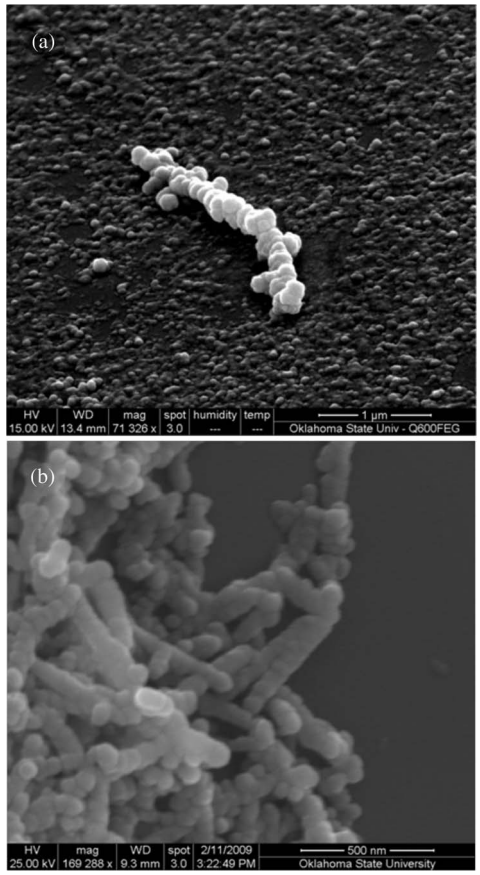

Fig. 2. High-resolution SEM images of (a) an isolated dendritic nanowire fragment (scale bar is 1 μm) and (b) typical high-density bunched dendritic nanowire region (scale bar is 500 nm), as found on the surface of the sphere seen in Fig. 1.

electrodes have been reduced, to 2 V at 10 Hz, resulting in the growth of a highly dendritic nanowire. The initial growth solution contained gold nanorods (purchased from Nanopartz) of an average aspect ratio of 4, confirmed by transmission electron microscope (TEM) imaging and absorption spectroscopy.After the nanowire was grown between the electrodes, precision stages were used to position the microsphere under the nanowire. The microsphere was then gently moved up through the electrode gap, breaking the nanowire free from the electrodes and positioning it on the surface of the microsphere. The result is shown in the SEM images of Fig. 1. The longer part of the nanowire, to the left in the images, is approximately along the sphere's equator. The shorter part to the right was probably displaced as the microsphere broke the surface of the growth solution. Note that the microsphere's stem makes a right-angle bend at a short distance from the microsphere; this is a consequence of the fabrication process.In use, the distant stem is held horizontally so that the near stem is vertical just below the sphere (actually, prolate spheroid), and defines its symmetry axis. The tapered fiber used for coupling is also horizontal, and tangent to the sphere. Two close-ups of nanowire regions are shown in Fig. 2.

The nanowire, as deposited on the surface of the microsphere, seen in Figs. 1 and 2, consists primarily of bunched dendritic segments of varying density, as in Fig. 2(b), along with isolated dendritic fragments, as in Fig. 2(a). Close-up images of the rest

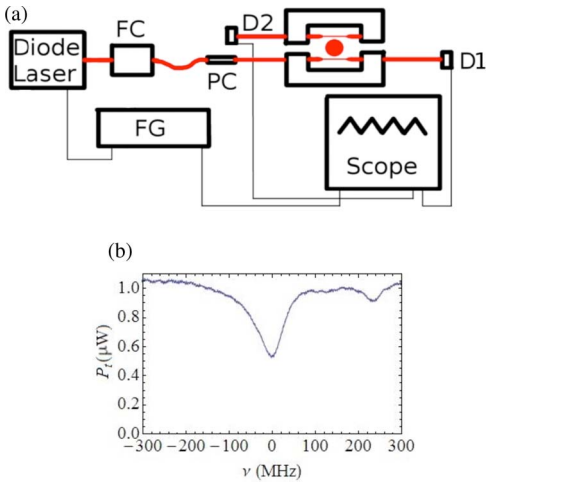

Fig. 3. (a) Simple schematic of the setup in which diode-laser light is evanescently coupled from a tapered fiber to the WGMs of a microsphere on which Au nanowires have been deposited. (b) Typical throughput power dip for a coated microsphere. The point of fiber–sphere contact is not on the nanowire.

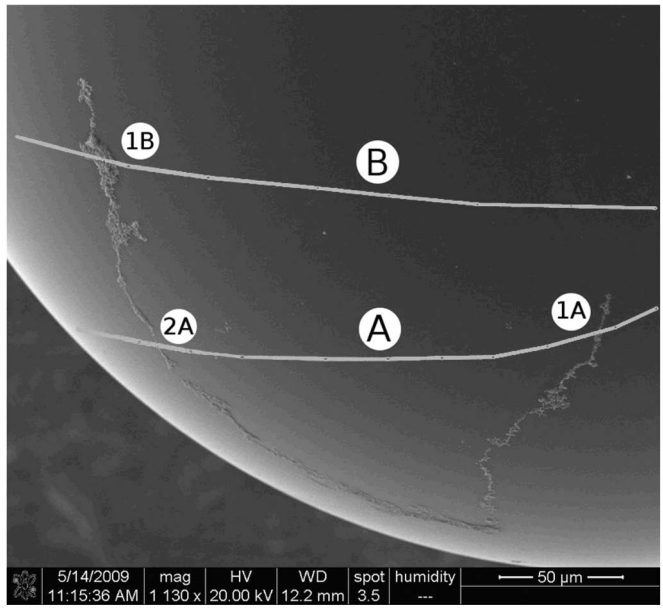

Fig. 4. Lines of longitude for two different paths (A, B) of probing the effect of the nanowire on evanescent coupling. The probe fiber is perpendicular to these paths and is brought into contact at points along each path. The main body of the nanowire is located at the equatorial plane of the microsphere (left side of the image). The scale bar is 50 μm.

of the surface show unchained gold nanorods, which were not incorporated into the nanowire in the dielectrophoretic process. The aspect ratio of an individual fragment is on average 10, with characteristic dimensions of about 500 nm $\times$ 50 nm as measured from the SEM images. The LSPRs of the fragments are optically excited, while the overall nanowire structure has a longitudinal LSPR that is too far into the infrared to be excited with telecommunication wavelengths. The longitudinal LSPR shifts to longer wavelengths with increasing aspect ratio [11]–[13]; with an aspect ratio of 13, the resonance is centered at 1550 nm and has a width of about 150 nm. Because the fragments are not single crystalline, there is additional LSPR broadening due to impedance losses at internal boundaries [14], [15]. The growth and deposition processes produce fragments with a distribution of aspect ratios that has a long tail toward high values, due to bunching. Thus, the effective resonance behavior is further broadened, and the near-field enhancement is reduced from what would be obtained if all fragments had the same aspect ratio. These effects are expected to limit the obtainable levels of useful enhancement as well as to contribute to scattering and absorption losses, in contrast to the case of the isolated and more nearly monodisperse Au nanorods used in previous studies [9].

III. Experiment and Analysis

A schematic of the basic setup involved in the experiment is shown in Fig. 3(a). Light from a tunable diode laser (New Focus model 6328) with a wavelength tuned around 1550 nm is linearly frequency scanned with an external function generator (FG). A fiber coupler (FC) launches the free-space laser beam into a single-mode optical fiber that has been tapered for microresonator coupling and mounted to a U-shaped holder. The holder is attached to a micrometer-controlled z-stage (translation axis normal to the plane of the figure, i.e., vertical) to enable latitude variation during spatial probing of the nanowire-coated microsphere. Light incident on the microresonator was either transverse electric (TE) or transverse magnetic (TM), linearly polarized with respect to the sphere's polarization basis (TE vertical, TM horizontal), with the polarization set by the polarization controller (PC). At the fiber output, a collimator and polarizing beam splitter (New Focus, 400:1 extinction ratio) were used to provide polarization analysis (D1 is a Newport model 818-IR detector). A portion of the throughput power spectrum from D1 is shown in Fig. 3(b).

A second tapered optical fiber is used as a probe (D2 is the same type of detector as D1) to increase the effective intrinsic loss, allowing determination of the coupling regime, as discussed in the following. The microsphere–fiber alignment is monitored from above with an optical microscope for measurement of the angle between the pump fiber and horizontal microsphere stem-–the longitude (θ). If z is defined to be the vertical distance from the upper (north) pole of the microsphere, the 2-D position data (z, θ) specify the latitude and longitude of the fiber–microsphere contact point, locating it with respect to the nanowire, as the coupling enhancement is spatially probed.

Prior to the application of the nanowire onto the surface of the microsphere, the surface was probed to determine the initial spatial variation of both coupling and intrinsic losses. Little z-variation is observed (losses increase slightly as the contact point nears the upper pole), and no θ-variation is observed. After application of the nanowire onto the surface of the microsphere, this procedure is repeated along two different lines of longitude separated by $\sim 32^\circ$, corresponding to two paths having distinct intersections with the nanowire, as seen in Fig. 4. With the initial and final values of the spatially dependent coupling and intrinsic losses determined, we then compute the ratios of both parameters, i.e., the coupling and intrinsic loss enhancements [9]; see analysis in the following.

Again, as the input light is scanned in frequency, dips in the detected throughput correspond to WGM resonances. The

WGMs are classified by the ratio $x = T/\alpha L$ of coupling loss T (probability of photon tunneling between WGM and fiber mode) to intrinsic loss αL (due to absorption and scattering), where α is the intrinsic loss coefficient and L is the microresonator circumference. A WGM with $x > 1$ is referred to as overcoupled, and one with $x < 1$ is called undercoupled. The loss ratio x determines the relative dip depth (which is also called extinction ratio) M_0 [5]

$$M_0 = \frac{4x}{(1+x)^2} \tag{1}$$

which is maximum ($M_0 = 1$, and throughput goes to zero) for critical coupling ($x = 1$).

Because a measured dip depth M_0 does not uniquely determine the loss ratio x, it is necessary to have a method for determining the coupling regime (undercoupled or overcoupled). Bringing a second fiber close to the microsphere effectively increases the intrinsic loss, changing the first fiber's throughput dip depth. Adding some extra loss makes the dip of an overcoupled mode deeper (M_0 increases), and that of an undercoupled mode shallower (M_0 decreases). With the knowledge of whether x is less than or greater than one, x can be uniquely determined from the measured M_0.

The enhancement factors for coupling and intrinsic loss can be found from measurements made on the throughput dip. Measurements of the depth and width of a dip give the quality factor Q and loss ratio x for that mode, provided that the coupling regime is known. Knowing Q and x before and after nanowire deposition is sufficient to determine both enhancement factors. To see this, consider the following expressions for the total (or loaded, i.e., including coupling loss T) Q of a WGM:

$$Q = \frac{\nu}{\Delta\nu} = \frac{2\pi n_{\text{eff}} L}{\lambda (T + \alpha L)} \tag{2}$$

where ν is the WGM frequency, $\Delta\nu$ the mode width, n_{eff} the effective index of refraction of the mode, L the microresonator circumference, λ the vacuum wavelength, and α the intrinsic loss coefficient. Note that $\Delta\nu$ and Q^{-1} are proportional to the total loss $T + \alpha L$; defining the coupling and intrinsic quality factors Q_c and Q_i to be similarly inversely proportional to T and αL, respectively, we have $Q^{-1} = Q_c^{-1} + Q_i^{-1}$. Using the definition of the loss ratio $x = T/\alpha L$ gives

$$\begin{aligned} Q_c &= Q\left(1 + \frac{1}{x}\right) \\ Q_i &= Q\,(1+x)\,. \end{aligned} \tag{3}$$

Now the coupling-enhancement factor can be found by comparing coupling losses before (T') and after (T'') depositing the nanowire on the surface of the resonator

$$F_c = \frac{T''}{T'} = \frac{Q_c'}{Q_c''} = \frac{Q'\,(1 + (1/x'))}{Q''\,(1 + (1/x''))} \tag{4}$$

and a similar ratio of the intrinsic losses before and after gives the intrinsic loss enhancement

$$F_i = \frac{\alpha'' L}{\alpha' L} = \frac{Q_i'}{Q_i''} = \frac{Q'\,(1+x')}{Q''\,(1+x'')}. \tag{5}$$

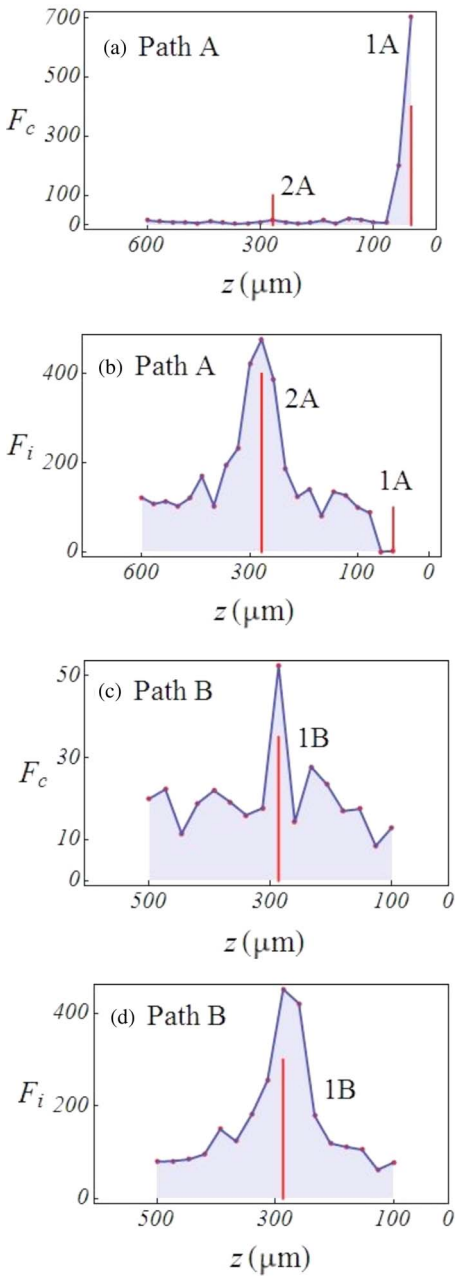

Fig. 5. Coupling enhancement F_c and intrinsic loss enhancement F_i measured for contact points along the two paths shown in Fig. 4. The upper (north) pole is at $z = 0$.

Note that the coupling enhancement given by (4) is not the same as a previously reported enhancement in extinction ratio [16].

IV. Results

The measured coupling enhancement F_c and intrinsic loss enhancement F_i are then correlated to SEM images of the microsphere using the 2-D positioning data taken experimentally. The enhancements that are found are plotted in Fig. 5 for each of the two paths shown in Fig. 4.

Along path B, we observe a mean evanescent coupling enhancement of a factor of roughly 10 when not in contact with the nanowire, and 55 when in contact (point 1B). The small enhancement seen, when not in contact, is a result of homogeneously distributed small Au fragments deposited during the nanowire placement. Along path A, we see a very large coupling enhancement ($\sim$700) at the location of the dislodged section of nanowire (point 1 A), and an enhancement at location 2 A that is similar to that seen at point 1B. The very high enhancement at location 1 A is due to a combination of low-density bunching and the local nanowire having broken free from the main body of the nanowire, so that the region with nanowire fragments between the sphere and the fiber is less extensive. The intrinsic loss enhancement has a weaker spatial dependence, as the optical path will encounter fragments acting as scatterers on the surface both above and below the equatorial plane. However, we find larger enhancement of loss near the equatorial plane, around $z = 300$ μm, as the optical path will encounter nearly the entire main body of the nanowire (about one-fourth of the circumference). For both paths A and B, we measure an intrinsic loss enhancement factor of $\sim$100 when not on the main equatorial nanowire, and a factor of $\sim$450 when on the main body of the nanowire. Further, it is found that as the source is detuned from the plasmon resonance band, the coupling enhancement, but not the intrinsic loss enhancement, falls off dramatically, even when the fiber is located in the nanowire region. Specifically, at 800 nm, the maximum coupling-enhancement factor is found to be approximately 4 for another nanowire-coated sphere having peak coupling enhancements of a factor of 600 at 1550 nm.

In comparison to earlier work presented in [9], where a low-aspect-ratio nanorod-coated microsphere had high coupling enhancement at 800 nm and weak enhancement at 1550 nm, the opposite is now true for a sphere coated with a nanowire—high enhancement at 1550 nm and weak enhancement at 800 nm. This implies that the longitudinal plasmon resonance has been shifted to longer wavelengths in the higher-aspect-ratio nanowire fragments, as predicted by theory [11]. Furthermore, the high localization of the peak coupling enhancement at the known position of the nanowire region is a clear indication of the effect of the nanowire on coupling and the relative shift in the plasmon resonance band. The strong wavelength dependence of the coupling enhancement indicates that this effect is tied to LSPR-related enhancement of the local evanescent fields.

V. Conclusion

In summary, we have demonstrated that Au nanowires coated on the surface of a high-Q microsphere lead to a surface-plasmon-assisted increase in evanescent coupling between the microsphere and a tapered optical fiber. We report plasmonic enhancement of evanescent optical coupling by factors of 10–700, as compared to the enhancement factors of 2–7 seen in [9] at this wavelength, $\sim$1550 nm. We further demonstrate localization of the peak enhancement of coupling to the known location of the Au nanowire with uncertainties of the order of the spatial extent of a WGM ($\sim$10 μm). Due to the structure and process of application of the nanowire to the microsphere, these enhancements of coupling are accompanied by large increases in intrinsic loss and scattering. These increases in loss can limit the usefulness of this particular process, as applied to microresonator-based evanescent sensors. However, with improvements in the nanowire-deposition process, these effects should largely be mitigated. The wavelength dependence of the coupling enhancement is clearly demonstrated, as at 800 nm, the peak-coupling-enhancement effect decreased by more than 99% with respect to the peak enhancement at 1550 nm, near the longitudinal plasmon resonance of the dendritic nanowire fragments. Our results at 1550 nm are comparable to the results of [9] at 800 nm.

Au nanowire-coated microresonators are expected to enhance the sensitivity of evanescent-wave chemical and gas sensors. The wavelength tunability of surface plasmon resonance peaks, by varying the aspect ratio, makes this a promising tool for various applications. These coated resonators can also be used for surface-enhanced Raman scattering experiments.

Acknowledgment

The authors would like to thank the staff of the Oklahoma State University Microscopy Laboratory for their assistance in the use of the electron microscopy facilities.

References

[1] A. K. Sharma, R. Jha, and B. D. Gupta, "Fiber-optic sensors based on surface plasmon resonance: A comprehensive review," *IEEE Sens. J.*, vol. 7, no. 8, pp. 1118–1129, Aug. 2007.

[2] A. K. Sharma and B. D. Gupta, "Fibre-optic sensor based on surface plasmon resonance with Ag–Au alloy nanoparticle films," *Nanotechnology*, vol. 17, no. 1, pp. 124–131, 2006.

[3] P. Stöcker, B. Menges, U. Langbein, and S. Mittler, "Multimode waveguide mode surface plasmon coupling: A sensitivity and device realizability study," *Sens. Actuators A*, vol. 116, no. 2, pp. 224–231, Oct. 2004.

[4] Y. C. Kim, W. Peng, S. Banerji, and K. S. Booksh, "Tapered fiber optic surface plasmon resonance sensor for analyses of vapor and liquid phases," *Opt. Lett.*, vol. 30, no. 17, pp. 2218–2220, 2005.

[5] A. T. Rosenberger, "Analysis of whispering-gallery microcavity-enhanced chemical absorption sensors," *Opt. Expr.*, vol. 15, no. 20, pp. 12959–12964, 2007.

[6] G. Farca, S. I. Shopova, and A. T. Rosenberger, "Cavity-enhanced laser absorption spectroscopy using microresonator whispering-gallery modes," *Opt. Expr.*, vol. 15, no. 25, pp. 17443–17448, 2007.

[7] N. M. Hanumegowda, C. J. Stica, B. C. Patel, I. White, and X. Fan, "Refractometric sensors based on microsphere resonators," *Appl. Phys. Lett.*, vol. 87, no. 20, pp. 201107-1–201107-3, 2005.

[8] M. Cai, G. Hunziker, and K. Vahala, "Fiber-optic add-drop device based on a silica microsphere whispering gallery mode system," *IEEE Photon. Technol. Lett.*, vol. 11, no. 6, pp. 686–687, Jun. 1999.

[9] S. I. Shopova, C. W. Blackledge, and A. T. Rosenberger, "Enhanced evanescent coupling to whispering-gallery modes due to gold nanorods grown on the microresonator surface," *Appl. Phys. B*, vol. 93, no. 1, pp. 183–187, 2008.

[10] B. Ozturk, C. Blackledge, B. N. Flanders, and D. R. Grischkowsky, "Reproducible interconnects assembled from gold nanorods," *Appl. Phys. Lett.*, vol. 88, no. 7, pp. 073108-1–073108-3, Feb. 2006.

[11] J. Pérez-Juste, I. Pastoriza-Santos, L. M. Liz-Marzán, and P. Mulvaney, "Gold nanorods: Synthesis, characterization and applications," *Coord. Chem. Rev.*, vol. 249, no. 17–18, pp. 1870–1901, 2005.

[12] N. R. Jana, L. Gearheart, and C. J. Murphy, "Seed-mediated growth approach for shape-controlled synthesis of spheroidal and rod-like gold nanoparticles using a surfactant template," *Adv. Mater.*, vol. 13, no. 18, pp. 1389–1393, 2001.

[13] B. P. Khanal and E. R. Zubarev, "Purification of high aspect ratio gold nanorods: Complete removal of platelets," *J. Amer. Chem. Soc.*, vol. 130, no. 38, pp. 12634–12635, 2008.
[14] C. Sönnichsen, T. Franzl, T. Wilk, G. von Plessen, and J. Feldmann, "Plasmon resonances in large noble-metal clusters," *New J. Phys.*, vol. 4, pp. 93-1–93-8, 2002.
[15] F. Neubrech, T. Kolb, R. Lovrincic, G. Fahsold, A. Pucci, J. Aizpurua, T. W. Cornelius, M. E. Toimil-Molares, R. Neumann, and S. Karim, "Resonances of individual metal nanowires in the infrared," *Appl. Phys. Lett.*, vol. 89, no. 25, pp. 253104-1–253104-3, 2006.
[16] N. K. Hon and A. W. Poon, "Surface plasmon resonance-assisted coupling to whispering-gallery modes in micropillar resonators," *J. Opt. Soc. Amer. B*, vol. 24, no. 8, pp. 1981–1986, 2007.

Elijah B. Dale received the B.S. and Ph.D. degrees, both in physics, from Oklahoma State University, Stillwater, in 2005 and 2010, respectively. His Ph.D. thesis was done under the supervision of Dr. A. T. Rosenberger.

He is currently a Staff Scientist with OEwaves, in Pasadena, CA. His current research interests, both experimental and theoretical, include optical microcavities with an emphasis on cavity coupling including optical plasmonics, polarization effects, and fundamental studies.

Deepak Ganta received the M.S. degree in electrical engineering, and the Ph.D. degree in photonics from Oklahoma State University, Stillwater, in 2002 and 2010, respectively. His Ph.D. thesis was done under the supervision of Dr. A. T. Rosenberger.

He is currently an Analytical Scientist with nGimat, in Atlanta, GA. His current research interests include nanomaterial synthesis, characterization, plasmonics, thin-film-based devices, and optical sensors.

Dr. Ganta is a member of the Optical Society of America and American Physical Society.

Deok-Jin Yu received the B.S. degree from Cheongju University, Cheongju, Korea, in 1996, and the M.S. degree from Chung-Ang University, Seoul, Korea, in 1998. He is currently working toward the Ph.D. degree at the Department of Physics, Oklahoma State University, Stillwater.

His current research interests include fabricating hybrid nanodevices of Au nanorods and single-walled carbon nanotubes, and Raman spectroscopy of nanomaterials.

Bret N. Flanders was born in Whittier, CA, in 1971. He received the B.S. degree in chemical physics from the University of California, San Diego, in 1993, and the Ph.D. degree in chemistry from the University of Chicago, Chicago, IL, in 1999.

From 2000 to 2002, he was a Postdoctoral Fellow at the University of Kansas, Lawrence. In 2002, he joined the Department of Physics, Oklahoma State University, Stillwater. He is currently an Associate Professor in the Department of Physics, Kansas State University, Manhattan. His research interests include synthesis and fundamental properties of nanoscale materials, with the aim of using these materials to interrogate the physiology of biological cells.

James P. Wicksted received the B.A. degree from New York University, New York, in 1975, and the M.A. and Ph.D. degrees from the City University of New York, New York, in 1978 and 1983, respectively.

In 1985, he became a member of the Department of Physics, Oklahoma State University, Stillwater, where he is currently a Full Professor and Head of the Department as well as a Noble Research Fellow in optical materials. His current research interests include the optical studies of various types of nanoparticle complexes that have potential biosensing and biomedical applications.

Dr. Wicksted is a member of the American Physical Society and the American Association for the Advancement of Science.

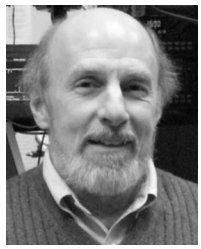

Albert T. Rosenberger (S'75–M'79) was born in Butte, MT. He received the B.A. degree in physics and mathematics from Whitman College, Walla Walla, WA, in 1971, the M.S. degree in physics from the University of Chicago, Chicago, IL, in 1972, and the Ph.D. degree in physics from the University of Illinois (Urbana-Champaign), Urbana, in 1979.

He is currently a Professor in the Department of Physics, Oklahoma State University, Stillwater. His current research interests include microresonator optics and plasmonics.

Dr. Rosenberger is a member of the American Physical Society (APS), the Optical Society of America, and the American Association of Physics Teachers, and was named an APS Outstanding Referee in 2008.